Supporting Information

Martin et al. 10.1073/pnas.1105816108

SI Methods

Reimagine Condition. During the scanning session, 45 reimagine trials were randomly interspersed. This condition (not analyzed as part of the current experiment) consisted of 45 previously constructed imagined future events. In the prescan session a week earlier, participants had constructed future events in response to experimenter-supplied generic person, place, and object cues. In the scanning session, participants were shown these cues and spent the 8-s trial imagining each already-constructed future event, followed by the same 4-s rating scale for detail.

MRI Acquisition. MRI data were collected on a Siemens Avanto 1.5 Tesla MRI scanner. For the anatomical scan, a magnetization-prepared rapidly acquired gradient echo (MP-RAGE) sequence was used, whereas the functional scans were collected with a T2*-weighted echo planar imaging (EPI) sequence (repetition time (TR) = 2,000 ms, echo time (TE) = 23 ms, matrix size = 64×64 , field of view (FOV) = 200 mm, flip angle = 90°). Twenty-five coronal oblique slices (5 mm thick) were acquired in an interleaved fashion, perpendicular to the long axis of the hippocampus and covering the whole brain. Five functional runs were acquired for each subject, with 270 time points per run (9 min). During the functional scans, the task stimuli were projected onto a screen in the scanner room and reflected into a mirror within the head coil. All participant responses were collected using a four-button response box.

Preprocessing of MRI Data. To allow the longitudinal magnetization to reach equilibrium, the initial four images from each run were discarded. The functional images were preprocessed using SPM8 (Wellcome Trust Centre for Neuroimaging, London, UK), correcting for slice timing differences, adjusting for movement across scans by realigning and unwarping, coregistering with the anatomical scan, normalizing (using normalization parameters derived during segmentation) the images to the Montreal Neurological Institute (MNI) template (resampled at $2 \times 2 \times 2$ mm voxels), and spatial smoothing with an 8-mm full-width half maximum Gaussian kernel. One participant's data contained some small movement artifacts; because a set of five trial-type sequences were generated with Optseq2 (1) and therefore 25 participants were required to maintain a complete counterbalance of these sequences, this participant's data were repaired via interpolation using ArtRepair Software (http://web.mit.edu/swg/ software.htm). The time-series functional (f)MRI data were high-pass filtered to account for low-frequency drifts; a cutoff value of 128 was used. An AR(1)-model was used to account for possible serial correlations.

Localization and Visualization of fMRI Activations. MNI coordinates of peak voxels were converted to Talairach space for the purposes of localization, and regions of activation were localized in reference to a standard stereotaxic atlas (2). Coordinates in all tables are reported in MNI space. For all figures, thresholded activation maps from SPM8 were overlaid on a standard anatomical template image (ch2better.nii) using in MRIcron (3). For those figures depicting activity from analyses focused on hippocampal activity, thresholded whole-brain maps were masked to show only voxels falling within the hippocampus (using an anatomical mask of the hippocampus from MARINA; ref. 4) and then overlaid on a standard anatomical template. Percentage of signal change data

were extracted from clusters of activation using the REX toolbox for SPM8. Note that as the option to plot group level parametric effects is not available in SPM8, a new fixed-effects model was used to compute percentage of signal change data for low detail (ratings 0–1) and high detail (ratings 2–3) future events. From each subject's first-level model, β -values (averaged across all active voxels within a 3-mm sphere) were extracted from each condition of interest in each run. These data were then converted to percentage of signal change by dividing by the value of the constant of that same run and multiplying by 100. Once rescaled, the percentage of signal change values for each condition from each run in that subject were averaged to create one value per condition per subject. These values were used to compute the mean percentage of signal change (and SE) for each condition of interest.

Functional Connectivity: Seed Partial Least Squares Analysis (PLS). PLS is a covariance-based multivariate technique that enables examination of connectivity between regions of interest ("seeds") and activity across the whole brain over time and whether there are similarities or differences in connectivity across experimental conditions (5–7). For this analysis, we extracted mean percentage of signal change (using REX as described above) from two seed regions within the right hippocampus (xyz = 20 - 12 - 16; 34 - 26 -8). These data were entered as seeds in the PLS analysis. First, correlations were computed between the signal in each seed region and all other voxels for each condition across subjects. The resulting correlation maps were stacked and analyzed with singular value decomposition, producing a set of orthogonal latent variables (LVs), each containing three matrices: (i) a singular value indicating the amount of covariance for which the LV accounts; (ii) a linear contrast between the seeds and the conditions that codes the effect depicted by voxels; and (iii) the singular image of voxel weights or "saliences" (akin to a component loadings in principle components analysis) that are proportional to the covariance of activity with the linear contrast. Each extracted latent variable successively accounted for a smaller portion of the covariance (as indicated by the singular value) and are thus determined by the strength of effects in the dataset.

The statistical significance of each LV was assessed by use of a permutation test. This procedure involved randomly reassigning each subject's data to experimental conditions, rerunning the PLS analysis, and determining the new singular value for each reordering; this was done 500 times. Thus, significance reflects the probability on the basis of the number of times the singular value from the permuted data exceeds the original singular value (7). A threshold of P < 0.05 was used. Note that unlike univariate analyses, the significance of whole-brain patterns of activity are determined in one single analytic step, and thus correcting for multiple comparisons is not necessary.

The reliability of the voxel saliences was computed using bootstrap estimation of the SE. This procedure involves randomly resampling subjects with replacement, rerunning the PLS analysis, and determining new saliences for each sampling. After carrying this procedure out 300 times, the SE of the saliences was computed (7). Clusters of five or more voxels in which bootstrap ratios were greater than ± 4.5 (roughly equal to a Z score, or a P value of P < 0.0001), were considered to represent reliable voxels.

- 1. Dale AM (1999) Optimal experimental design for event-related fMRI. *Hum Brain Mapp* 8:109–114.
- Talaraich J, Tournoux P (1988) Co-Planar Stereotaxic Atlas of the Human Brain (Thieme, New York).
- 3. Rorden C, Karnath HO, Bonilha L (2007) Improving lesion-symptom mapping. *J Cogn Neurosci* 19:1081–1088.
- Walter B, et al. (2003) MARINA: An easy to use tool for the creation of MAsks for Region of INterest Analyses. In: 9th International Conference on Functional Mapping of the Human Brain. New York. NY.
- McIntosh AR, Chau WK, Protzner AB (2004) Spatiotemporal analysis of event-related fMRI data using partial least squares. Neuroimage 23:764–775.
- McIntosh AR, Lobaugh NJ (2004) Partial least squares analysis of neuroimaging data: Applications and advances. Neuroimage 23(Suppl 1):S250–S263.
- McIntosh AR, Bookstein FL, Haxby JV, Grady CL (1996) Spatial pattern analysis of functional brain images using partial least squares. Neuroimage 3:143–157.

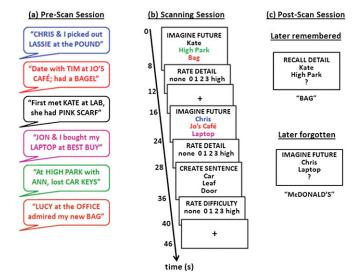


Fig. S1. Future simulation paradigm. During the prescan session (A), participants retrieved episodic memories and identified a person, place, and object featuring in each. Sets of rearranged memory details were presented during scanning (B); for each, the participant imagined a future event including all three details and rated the simulation for detail. On control trials, three objects were presented, and participants created a "size sentence," ordering the objects by physical size, and rated the difficulty of this task. In the postscan session (C), participants completed a cued-recall test. For each detail set presented during scanning, two memory details were provided, and if the third detail was correctly recalled, the relevant simulation trial (from the fMRI scan) was classified as "later remembered"; if incorrect, the relevant simulation trial was classified as "later forgotten."

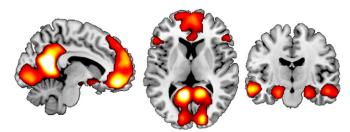


Fig. 52. Regions engaged by imagining future events. The contrast of future events (collapsed across encoding success) relative to control trials revealed activation of the core network, including bilateral medial parietal and prefrontal cortices (Left and Middle) and bilateral medial temporal lobes and left lateral temporal cortex (Right). Activations are shown at a voxelwise threshold of P < 0.005 uncorrected and an extent threshold of 145 voxels, providing correction for multiple comparisons at P < 0.05.

Table S1. Regions activated by imagining future events relative to the control condition

MNI coordinates Brain region Z score P value х z 27,892* L retrosplenial/posterior cingulate cortex (BA 31) -8 -56 20 Inf < 0.001 R lingual gyrus (BA 17) 16 -88 2 Inf < 0.001 L inferior temporal gyrus (BA 21) -58 -6 -18Inf < 0.001 R middle temporal gyrus (BA 21) 58 -6 -20< 0.001 Inf L lingual gyrus (BA 17) -14-88 0 Inf < 0.001 L medial frontal gyrus (BA 10/11) -8 46 -12 Inf < 0.001 L medial frontal gyrus (BA 8) -22 24 42 < 0.001 Inf L medial frontal gyrus (BA 9) -6 56 22 Inf < 0.001 R parahippocampal gyrus (BA 35/36) 28 < 0.001 -28 -18 6.47 R parahippocampal gyrus (BA 28) -14-22 6.31 < 0.001 -22 L temporal pole (BA 38) -46 12 -34 6.13 < 0.001 L inferior frontal gyrus (BA 47) -32 -16 6.05 <0.001 30 L parahippocampal gyrus (BA 36) -24 -36 -145.98 < 0.001 R hippocampus 26 -18 -205.93 < 0.001 R temporal pole (BA 38) 48 14 -325.51 < 0.001 R superior frontal gyrus (BA 9) 12 4.82 < 0.001 52 40 1,589 L angular gyrus (BA 39) < 0.001 -46 -7032 Inf 1,228 R inferior frontal gyrus (BA 47) 36 32 5.01 <0.001 -14R inferior frontal gyrus (BA 46/45) 52 28 16 4.98 < 0.001 795 R angular gyrus (BA 39) 50 -6226 6.62 <0.001

All clusters are significant at P < 0.05, corrected for multiple comparisons. Infinite Z scores are due to the P value being so small that the Z score is effectively infinite. Cluster size (k) indicates the number of voxels comprising the cluster; only clusters with a minimum extent of 145 voxels are reported. Voxel-level P value is provided. BA, Brodmann area; MNI, Montreal Neurological Institute; Inf, infinite; L, left; R, right. *Cluster extends bilaterally.